The g-factors and magnetic rotation in ^{82}Rb*

Yuan Da-Qing(袁大庆), Zheng Yong-Nan(郑永男), Zuo Yi(左 翼), Fan Ping(范 平), Zhou Dong-Mei(周冬梅), Wu Xiao-Guang(吴晓光), Zhu Li-Hua(竺礼华), Li Guang-Sheng(李广生), Xu Guo-Ji(许国基), Fan Qi-Wen(樊启文), Zhang Xi-Zhen(张锡珍), and Zhu Sheng-Yun(朱升云)†

China Institute of Atomic Energy, Beijing 102413, *China*

(Received 24 December 2008; revised manuscript received 12 October 2009)

The g-factors of the intra-band states 12, 13, 14, 15 in a magnetic-rotational band built on the 11 state in ^{82}Rb are measured for the first time by using a transient magnetic field-ion implantation perturbed angular distribution (TMF-IMPAD) method. The magnetic-rotational band in ^{82}Rb is populated by the ^{60}Ni(^{27}Al,4pn)^{82}Rb reaction, and the time-integral Larmor precessions are measured after recoil implantation into a polarized Fe foil. The calculation of g-factors is also carried out in terms of a semi-classical model of independent particle angular momentum coupling on the basis of the four-quasiparticle configuration $\pi(g_{9/2})^2 \otimes \pi(p_{3/2}, f_{5/2}) \otimes \nu\left(g_{9/2}\right)$. The measured and calculated g-factors are in good agreement with each other. The g-factors and deduced shear angles decrease with the increase of spin along the band. This clearly illustrates the shear effect of a step-by-step alignment of the valence protons and neutrons in magnetic rotation. The semi-classical calculation also shows that the alignment of the valence neutron angular momentum is faster than that of the valence protons, which results in a decrease of g-factors with increasing spin. The present results provide solid evidence of the shear mechanism of magnetic rotation.

Keywords: ^{82}Rb, magnetic rotation, g-factor, TMF-IMPAD
PACC: 2750, 2110K, 2190

1. Introduction

Magnetic rotation, which was first found in Pb isotopes,[1] is a novel mode of nuclear rotation occurring in nuclei of nearly spherical shape. Understanding of its nature has attracted great interest in nuclear structure studies at high spins.[2] The magnetic-rotational band is characterized by magnetic dipole (M1) transitions with crossover E2 transitions very weak or absent. In addition, the magnetic-rotational band is associated with a rather small dynamical moment of inertia and its band-head occupies a high K value, implying multi-quasiparticle configurations.[3] The angular momentum vector of a valence proton particle is perpendicular to that of a valence neutron hole at the band head in Pb isotopes.[4] The resultant proton and neutron vectors form two blades of a pair of shears, and the total angular momentum increases by closing the shear blades along the band. The perpendicular coupling of the high j particle and hole orbitals at the band head results in a large transverse component $\mu_\perp$ of the magnetic moment vector that rotates around the total angular momentum. The energy and the angular momentum increase with the decrease of the angle between particle and hole spins. As the spins of the particle and hole are fully aligned, a highest-spin state is formed and the band is terminated.

Since the magnetic-rotation band resembles the closing of the two blades along the band it is called the shear band.[5] The shear band was investigated theoretically by the tilted axis cranking (TAC) model[6] and by the residual interaction between proton and neutron.[7]

The shear mechanism of a step-by-step alignment of the angular momenta of a high-spin particle and hole can be well studied through electromagnetic properties, such as the B(M1) transition strength and g-factor. So far, the shear band or shear mechanism has been investigated mostly by measuring the lifetimes of magnetic-rotational states.[2] The B(M1) transition strength deduced from the lifetime has played a role in studying magnetic rotation. However, the derived B(M1) value depends on the perpendicular component of the magnetic moment vector, since the g-factor depends on the parallel component of the magnetic moment vector with respect to the an-

*Project supported by the National Natural Science Foundation of China (Grant Nos. 10435010 and 10375093).

†Corresponding author. E-mail: zhusy@ciae.ac.cn

© 2010 Chinese Physical Society and IOP Publishing Ltd

gular momentum direction. The measurement of both these components can reveal the full coupling scheme and the configuration of the shear states.[2]

^{82}Rb ($Z = 37$, $N = 45$) lies in a mass region of transition from deformed to spherical shapes. At a neutron number of 45, the intruder $g_{9/2}$ sub-shell is half-filled and has already lost most of the capability to induce deformation. The competition between the deformation driving $g_{9/2}$ valence proton excitations and the almost spherical $g_{9/2}$ valence neutron excitations results in a moderate small deformation in ^{82}Rb.[8] Therefore, this nucleus is particularly suitable for the study of magnetic rotation. The magnetic-rotational band in ^{82}Rb was observed by Schnare *et al.*,[9] Schwengner *et al.*[10] and Döring *et al.*[11] Figure 1 shows the decay scheme of the negative parity $I = 1$ magnetic-rotational band built on the 11^- state in ^{82}Rb. The g-factors are very sensitive to the alignments of the valence proton and valence neutron due to different signs and magnitudes of the $g_{9/2}$ proton and neutron and are expected to vary systematically in magnetic rotation as the shears turn close or the spin goes up. Therefore, g-factors of intra-band states can provide direct evidence of the shear mechanism of magnetic rotation.

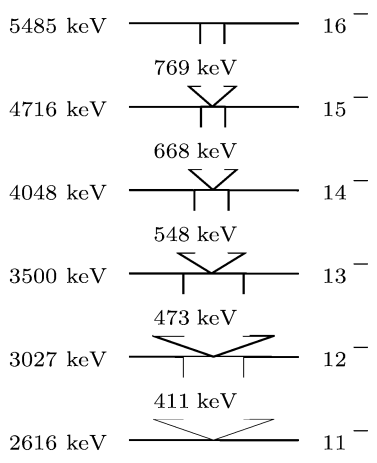


Fig. 1. Level scheme of the ^{82}Rb magnetic-rotational band cited from Refs. [10] and [11].

In order to investigate the coupling scheme between proton angular momentum and neutron angular momentum and the shear mechanism, the g-factors of four intra-band states of magnetic rotation in ^{82}Rb are measured for the first time by the transient magnetic field-ion implantation perturbed angular distribution (TMF-IMPAD) method[12,13] and calculated by a semi-classical model on the basis of independent particle angular momentum coupling.[7]

2. Experimental details

The g-factors of the high spin states for the magnetic-rotational band built on the 11^- state in ^{82}Rb were determined by a transient magnetic field-ion implantation perturbed angular distribution (TMF-IMPAD) method. The magnetic-rotational states in ^{82}Rb were populated by the fusion–evaporation reaction ^{60}Ni(^{27}Al,4pn)^{82}Rb with a 130-MeV Al beam from the HI-13 tandem accelerator at the China Institute of Atomic Energy. This reaction with a heavier projectile ^{27}Al brought in the higher recoil energy of ^{82}Rb required by the TMF-IMPAD method. The reaction cross section calculated with the PACE4 program[14] is ~ 4 mb at 130 MeV.

A schematic drawing of the TMF-IMPAD set-up is shown in Fig. 2. It is mainly composed of the target chamber housing a three-layer target assembly, the polarizing electromagnet and the γ-ray detector system.[12] The "T" shaped bronze target chamber was located between the two pole tips of the polarizing electromagnet. The three layer target assembly of ^{60}Ni–Fe–Cu was made in such a way that a 0.439-mg·cm^{-2} target layer of ^{60}Ni enriched to 99.6% was evaporated onto an annealed natural Fe layer of 1.51-mg·cm^{-2}, on whose other side a Cu stopper layer of 12-mg·cm^{-2} was evaporated and the assembly was then annealed to make the cubic Cu stopper layer defect-free. A Ta beam stopper was situated inside the chamber at 2 mm away from the target in the down stream. The ^{82}Rb recoiling nucleus with an average velocity of 0.028–0.029C passed through the Fe layer in a traverse time of 0.35 ps and stopped in the Cu stopper layer. The ferromagnetic Fe layer was polarized by a 0.16-T magnetic field, whose direction was perpendicular to the beam–detector plane and reversed up and down every 120 s during the measurement. The field changed its direction (up or down) by a field direction controller of the electromagnet, which generated positive pulse signals synchronically. As the ^{82}Rb nucleus moved along the polarized Fe layer, it experienced a transient magnetic field of $\sim 1.56 \times 10^3$ T, and nuclear precession about the direction of the polarizing magnetic field took place. The nucleus completed its decay to the ground state in the perturbation-free Cu stopper. The emitted γ rays were detected by four BGO Compton suppressed HPGe detectors with an efficiency of $\sim$30%. The four detectors were placed in the beam–detector plane at $\theta_1 \pm 60°$ and $\theta_2 \pm 120°$ with respect to the beam direction. The two-fold γ–γ coincidence data were recorded

in a five-parameter event-by-event mode with a Kodaq data acquisition system.[15] The five parameters are specified by the polarizing field direction and the 4 γ-ray detectors.

In data analysis, the γ–γ coincidence data of each detector with the other three detectors generated three matrices for each polarizing field direction. The γ ray counts of interest $N(\theta)$ were obtained as a geometric mean value of a series of spectra from different matrices or different gates.

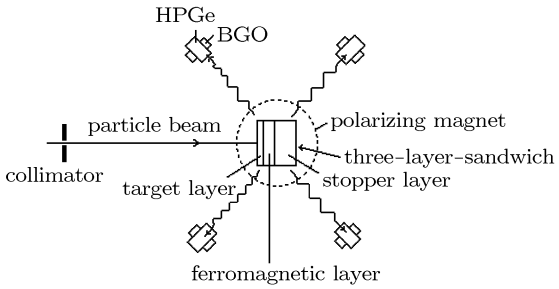


Fig. 2. Schematic drawing of the TMF-IMPAD set-up.

The nuclear precession of a state was inferred from a double ratio ρ obtained through the single ratios $\rho(\pm\theta_{\rm i})$ formed with the counting rates of an adjacent pair of detectors at $\pm\theta_{\rm i}$ for an observed transition.[12,16]

The single ratios are given as

$$\rho(\pm\theta_1) = \left(\frac{N(+\theta_1)\uparrow \times N(-\theta_1)\downarrow}{N(+\theta_1)\downarrow \times N(-\theta_1)\uparrow}\right)^{1/2},$$
$$\rho(\pm\theta_2) = \left(\frac{N(+\theta_2)\uparrow \times N(-\theta_2)\downarrow}{N(+\theta_2)\downarrow \times N(-\theta_2)\uparrow}\right)^{1/2}, \quad (1)$$

where $N(\theta_{\rm i})$ is the γ-ray count of interest, detected by a detector located at $\theta_{\rm i}$, and the arrows $\uparrow$ and $\downarrow$ specify the field up and down directions of the polarizing magnetic field, respectively. The double ratio is defined as

$$\rho = \left(\frac{\rho(\pm\theta_2)}{\rho(\pm\theta_1)}\right)^{1/2}. \quad (2)$$

Then, the precession angle $\Delta\phi$ can be obtained by

$$\Delta\phi = \varepsilon/S(\theta), \quad (3)$$

where the term ε is an experimental ratio defined as

$$\varepsilon = \frac{\rho-1}{\rho+1}, \quad (4)$$

and $S(\theta)$ is the logarithmic slope of γ-ray angular distribution

$$S(\theta) = \frac{1}{W(\theta)}\frac{{\rm d}W(\theta)}{{\rm d}\theta}. \quad (5)$$

The angular distributions were measured experimentally by shifting the four detectors 10° from the measurement geometry, so that γ-ray counts at 8 positions , $\theta_1\pm60°$ and $\theta_2\pm120°$ and θ_1=+70° and −50° and θ_2=+130° and −110° were obtained. After the γ-ray counts were normalized to the beam current and the detector efficiency, the coefficients of A_2 and A_4 were extracted by fitting the measured angular distributions.

The precession angle $\Delta\phi$ depends on the nuclear g factor and transient magnetic field strength $B_{\rm TMF}(t)$ experienced by a nucleus as follows:

$$\Delta\phi = -(g\mu_{\rm N}/\hbar)\int_{\rm en}^{\rm ex} B_{\rm TMF}(t){\rm e}^{-t/\tau}{\rm d}t, \quad (6)$$

where $\mu_{\rm N}$ is the nuclear magneton and τ is the mean lifetime of the nuclear state. The transient magnetic field $B_{\rm TMF}(t)$ is given by Shu's parametrization[17]

$$B_{\rm TMF}(\nu) = 96.7(v/v_0)^{0.45}Z^{1.1}\mu_{\rm B}N_{\rm p}, \quad (7)$$

where v_0 is the Bohr velocity, v is the velocity of a recoiling nucleus, $\mu_{\rm B}$ is the Bohr magneton and $N_{\rm p}$ is the number of polarized electrons in unit volume (for Fe, $N_{\rm p}$ is 2.22). The $B_{\rm TMF}(v)$ depends on the instantaneous velocity v of the recoiling nucleus in the Fe layer. The integration of Eq. (7) runs over the time period when the recoiling nucleus enters into and exits from the ferromagnetic Fe layer. Then, the g-factor for a given nuclear state can be obtained from Eqs. (3) and (6).

In data reduction the precession transfer was taken into account. The precession of a lower state also includes the precessions of higher spin states in cascade transitions and side feeding states, therefore it is an algebraic sum of precessions of itself and all states that feed it. The correction of the precession transfer was made according to

$$\varepsilon_{ij} = \sum_{l=i}^{N}\varepsilon_{ij}^{l}Y_{ij}^{l}, \quad (8)$$

where ε_{ij} is the experimental value in terms of Eq. (4) from the i state to the j state, Y is the relative intensity of decay from the l state to the j state; the summation runs over all decay paths to the j state.[18] The net precession angle was calculated using Eq. (3) with ε_{ij}^{i} obtained from Eq. (8). A computer program for precession transfer correction was written and used to obtain the net precession of the given state.

3. Results and discussion

Table 1 lists the magnetic-rotational states in ^{82}Rb and their lifetimes, logarithmic slope S of γ-ray angular distribution calculated from the measured angle distribution, experimentally measured and precession transfer corrected ε, net precession angle and g-factor in ^{82}Rb.

Table 1. Measured g-factors and corresponding parameters for ^{82}Rb.

state	life time/ps[a]	S	experimentally measured ε	precession transfer corrected ε	net precession angle/mrad	g-factor
12^-	0.58(11)	0.3149	0.005198	0.006840	21.72	1.12
13^-	0.59(11)	0.3149	0.004798	0.006312	20.05	1.03
14^-	0.37(6)	0.2904	0.004372	0.004229	14.56	0.866
15^-	< 1	0.2535	0.004485	0.004485	17.69	0.816

[a] from Ref. [10].

The 15^- state was the highest state observed in the present experiment and, therefore, the correction of precession transfer was not made. Since the ion traverse time in the Fe layer is ∼0.35 ps, the relative change of the integral part of Eq. (6) is 15% only with lifetime changing from 0.5 ps to 1 ps. So the uncertainty due to the lifetime is expected to be 5%. The mean traverse time of recoiling ^{82}Rb in the Ni target layer is less than 0.05 ps and the transient magnetic field $B_{\rm TMF}$ in Ni is 30% of that in Fe, so the precession angle induced by the transient magnetic field in Ni is negligible. Table 2 shows the sources of experimental uncertainties.

Table 2. Sources of uncertainties.

source of uncertainty	relative uncertainty
double ratio	1%
lifetime	5%
correction of precession transfer	18%
transient magnetic field	10%
S value	10%
combined standard uncertainty	25%

A semi-classical model based on the independent particle angular momentum coupling was used to calculate the g-factors and shear angles of the intra-band states and to examine the configuration.[7,8] Figure 3 shows the coupling scheme between neutron and proton angular momenta in magnetic rotation. Parameters θ_π and θ_ν are the angles of the proton vector and the neutron vector with respect to the total angular momentum that is $\boldsymbol{I} = \boldsymbol{j}_\pi + \boldsymbol{j}_\nu$, because the contribution of small deformation to the rotation is negligible. The shear or blade angle θ for a given state in the M1 band with $\Delta I = 1$ can be deduced using Eq. (9)

$$\cos\theta = \frac{\boldsymbol{j}_\nu \cdot \boldsymbol{j}_\pi}{|\boldsymbol{j}_\nu||\boldsymbol{j}_\pi|} = [I(I+1) - j_\nu(j_\nu+1) - j_\pi(j_\pi+1)]/2[j_\nu(j_\nu+1)j_\pi(j_\pi+1)]^{1/2}, \quad (9)$$

where $\theta_\nu = \theta - \theta_\pi$ and $\tan\theta_\pi = j_\nu \sin\theta / (j_\pi + j_\nu \cos\theta)$.

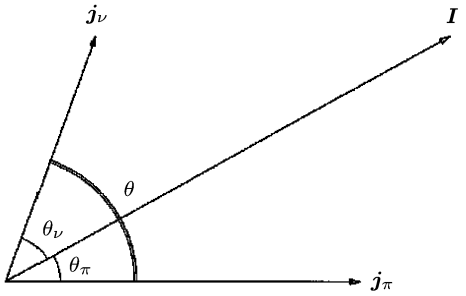


Fig. 3. Angular momentum coupling between neutron and proton vectors.

The magnetic moment is given by

$$\mu = gI = \frac{1}{\mu_0} \langle JJ|\, M_Z|\, JJ\rangle . \quad (10)$$

Taking into account the collective rotation with angular momentum $\boldsymbol{R}$, the total angular momentum is $\boldsymbol{I} = \boldsymbol{j}_\pi + \boldsymbol{j}_\nu + \boldsymbol{R}$ and then $M = g_\nu \bar{j}_\nu + g_\pi \boldsymbol{j}_\pi + g_R \boldsymbol{R}$. Thus,

$$gI = \langle II|M_Z|II\rangle = \frac{1}{I+1}\langle II|\boldsymbol{M}\cdot\boldsymbol{I}|II\rangle = \frac{1}{I+1}(g_\nu \boldsymbol{j}_\nu \cdot \boldsymbol{I} + g_\pi \boldsymbol{j}_\pi \cdot \boldsymbol{I} + g_R \boldsymbol{R}\cdot\boldsymbol{I}), \quad (11)$$

$$g = \frac{1}{I+1}\left(g_\nu j_\nu \cos\theta_\nu + g_\pi j_\pi \cos\theta_\pi + g_R R\right), \quad (12)$$

where g_R is the g-factor for collective rotation, which is close to Z/A. The contribution from collective rotation is neglected in magnetic rotation. Therefore, the

g-factor is expressed as

$$g = \frac{1}{I+1}\left(g_\nu j_\nu \cos\theta_\nu + g_\pi j_\pi \cos\theta_\pi\right). \qquad (13)$$

Reference [19] gave the effective g-factors for protons and neutrons respectively

$$g_s^{\rm eff}(\pi,\nu) \approx 0.75 \times g_s^{\rm free}(\pi,\nu) \quad \text{and}$$
$$g_l^{\rm eff} \approx 1.1 \ \text{ or } \ -0.1. \qquad (14)$$

Both the TAC calculations by Schnare *et al.*[9] and Schwengner *et al.*[10] on the basis of the four-quasiparticle (4qp) configuration $\pi(fp)\otimes\pi(g_{9/2})^2\otimes\nu(g_{9/2})$ and the Hartree–Fock–Bogoliubov shape calculations by Döring *et al.*[11] indicate that all magnetic-rotational states in ^{82}Rb are γ soft states with a small equilibrium deformation. In view of the spins, the configuration may be 4qp states in the spin range 11^-, 12^-, 13^-, 14^-, and 15^-, which are formed by 2 qp states $\pi(g_{9/2})\otimes\nu(g_{9/2})_{6+,7+,8+,9+}$ coupled to a cluster of $(p_{3/2},g_{9/2})$ or $(f_{5/2},g_{9/2})$ with spin 5 or 6. This reveals the shear mechanism in which the step-by-step alignment is generated by the coupling of a $g_{9/2}$ proton and a $g_{9/2}$ neutron.[9,10] From the viewpoint of the residual interaction between protons and neutrons[7] and the perpendicular angular momentum vectors of high j protons and neutrons at the band head of magnetic rotation, it follows that the perpendicular angular momentum vectors of $\pi(g_{9/2})^2$ and $\nu(g_{9/2})$ can be realized only in the case where one $p_{3/2}$ or $f_{5/2}$ proton is fully aligned and the shear band is generated by the coupling of two protons in the $g_{9/2}$ orbit and one unpaired $g_{9/2}$ neutron. Then, the calculation of the g-factors of magnetic-rotational states in ^{82}Rb was carried out by means of Eq. (9) for two configurations $\pi(p_{3/2})\otimes\pi(g_{9/2})^2\otimes\nu(g_{9/2})$ and $\pi(f_{5/2})\otimes\pi(g_{9/2})^2\otimes\nu(g_{9/2})$. Figure 4 shows the measured and calculated g-factors.

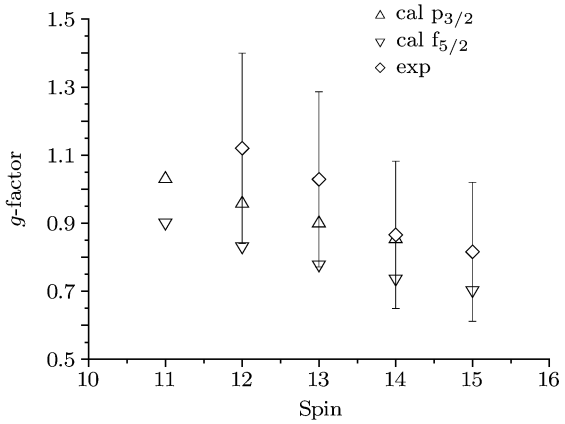


Fig. 4. Measured and calculated g-factors of magnetic-rotational states in ^{82}Rb.

The calculated and measured g-factors are in agreement within the experimental error, and both of them decline with the increase of spin along the band. Note that the configuration $\pi(p_{3/2})\otimes\pi(g_{9/2})^2\otimes\nu(g_{9/2})$ gives g-factors up to spin 14 only.

As shown in Fig. 5, the calculated values of shear angle θ between $\boldsymbol{j}_\pi$ (two $g_{9/2}$ protons) and $\boldsymbol{j}_\nu$ (one unpaired $g_{9/2}$ neutron) decrease with spin increasing along the band and the shear angle at the band-head is 88° on the basis of the configuration $\pi(p_{3/2})\otimes\pi(g_{9/2})^2\otimes\nu(g_{9/2})$. The calculated angle θ_π between the high j proton angular momentum and the total angular momentum is also shown in Fig. 5. The decreasing of the angle θ_π with the increase of spin is slower than that of the shear angle θ. This means that the angle θ_ν between the valence neutron angular momentum and the total angular momentum makes a major contribution to the change of shear angle, i.e., the valence neutron alignment towards the total angular momentum is much faster than the proton alignment. This rapid alignment of valence neutrons leads to a reduction of g-factors with spin increasing along the band. The decreasing of both g-factors and shear angles with increasing spin provides strong evidence that the angular momentum along the magnetic-rotational band is generated by the shear effects of a step-by-step alignment of the high-spin valence protons and neutrons.

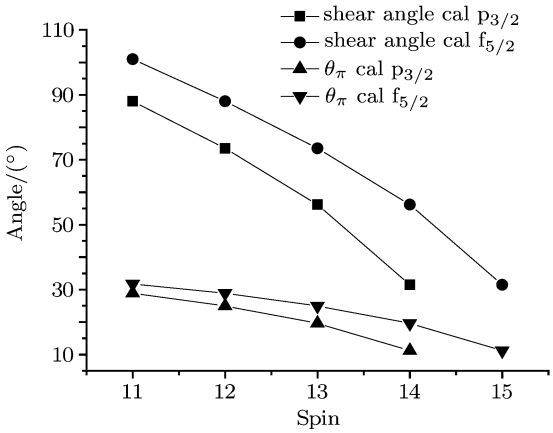


Fig. 5. Variations of shear angles θ and θ_π with spin increasing along the magnetic-rotational band in ^{82}Rb.

4. Conclusion

The g-factors of the 4 intra-band states along the magnetic-rotational band built on the 11^- state in ^{82}Rb are measured for the first time by using the TMF–IMPAD method. The g-factors are also calcu-

lated by a semi-classical model of the independent particle angular momentum coupling assumption on the basis of the 4 qp configuration $\pi(g_{9/2})^2_{\otimes}\pi(p_{3/2}, f_{5/2}) \otimes \nu(g_{9/2})$. Both g-factors and shear angles decrease with the increase of spin in the band, illustrating clearly that the angular momentum along the magnetic-rotational band is generated by the shear effects of a step-by-step alignment of the high-spin valence protons and neutrons. The fast alignment of the valence neutron angular momentum towards the total angular momentum leads to a decrease of the g-factors along the band. The present experimental results provide solid evidence for the shear mechanism of magnetic rotation.

References

[1] Neffgen M, Baldsiefen G, Frauendörf S, Grawe H, Heese J, Hübel H, Kluge H, Korichi A, Korten W, Maier K H, Mehta D, Meng J, Nenoff N, Piiparinen M, Schönhofer M, Schubart R, van Severen U J, Singh N, Sletten G, Thirumala Rao B V and Willsau P 1995 *Nucl. Phys.* A **595** 499

[2] Hübel H 2005 *Progr. Part. Nucl. Phys.* **54** 1

[3] Datta P, Chattopadhyay S, Banerjeeet P, Bhattacharya S, Dasmahapatra B, Ghosh T K, Goswami A, Pal S, Saha Sarkar M, Sen H S, Jain C, Joshi P K and Amita 2004 *Phys. Rev.* C **69** 044317

[4] Chmel S, Brandolini F, Ribas R V, Baldsiefen G, Görgen A, De Poli M, Pavan P and Hübel H 1997 *Phys. Rev. Lett.* **79** 2002

[5] Baldsiefen G, Hübel H, Korten W, Mehta D, Nenoff N, Thirumala Rao B V, Willsau P, Grawe H, Heese J, Kluge H, Maier K H, Schubart R, Frauendorf S and Maier H J 1994 *Nucl. Phys.* A **574** 521

[6] Frauendorf S 2001 *Rev. Mod. Phys.* **73** 463

[7] Macchiavelli A O, Clark R M, Fallon P, Deleplanque M A, Diamond R M, Krücken R, Lee I Y, Stephens F S, Asztalos S and Vetter K 1998 *Phys. Rev.* C **57** R1073

[8] Clark R M and Macchiavelli A O 2000 *Ann. Rev. Nucl. Part. Sci.* **50** 1

[9] Schnare H, Schwengner R, Frauendorf S, Dönau F, Käubler L, Prade H, Jungclaus A, Lieb K P, Lingk C, Skoda S, Eberth J, de Angelis G, Gadea A, Farnea E, Napoli D R, Ur C A and Lo Bianco G 1999 *Phys. Rev. Lett.* **82** 4408

[10] Schwengner R, Rainovski G, Schnare H, Wagner A, Dönau F, Jungclaus A, Hausmann M, Iordanov O, Lieb K P, Napoli D R, de Angelis G, Axiotis M, Marginean N, Brandolini F and Rossi Alvarez C 2002 *Phys. Rev.* C **66** 024310

[11] Döring J, Ulrich D, Johns G D, Johns G D, Riley M A and Tabor S L 1999 *Phys. Rev.* C **59** 71

[12] Zhu S Y, Luo O, Gou Z H, Zheng S G, Fan Z G, Li A L, Li G S, Wen S X, Dai Z Y, Liu X G and Wu X G 1996 *Chin. J. Nucl. Phys.* **18** 171

[13] Zhu S Y, Luo O, Li G S, Fan Z G, Xu Y J, Gao Z C, Wen S X, Wu X G, Liu X G, Xu G J, Zhu J Z, Chen Y S, Matsuta K, Fukuda M, Mihara M and Minamisono T 2000 *Chin. Phys. Lett.* **17** 560

[14] Tarasov O B and Bazin D 2003 *Nucl. Inst. & Meth. Phys. Res.* B **204** 174

[15] Omata K, Fujita Y, Yoshikawa N, Sekiguchi M and Shida Y 1991 *Proc. IEEE 7th Real Time '91 on Computer Applications in Nuclear, Particle and Plasma Physics* Jülich, p. 243

[16] Benczer-Koller, Hass N and Sak J 1980 *Ann. Rec. Nucl. Part. Sci.* **30** 53

[17] Shu N K B, Melnik D, Brennan J M, Brennan J M, Semmler W and Benczer-Koller N 1980 *Phys. Rev.* C **21** 1828

[18] Ribas R V 1993 *Nucl. Instr. & Methods* A **328** 553

[19] Speidl K H, Kenn O and Nowacki F 2005 *Progr. Part. Nucl. Phys.* **49** 91